Multi-Joint Coordination During Walking and Foothold Searching in the *Blaberus* Cockroach. II. Extensor Motor Neuron Pattern

ANDREW K. TRYBA AND ROY E. RITZMANN
Department of Biology, Case Western Reserve University, Cleveland, Ohio 44106-7080

Tryba, Andrew K. and Roy E. Ritzmann. Multi-joint coordination during walking and foothold searching in the *Blaberus* cockroach. II. Extensor motor neuron pattern. *J Neurophysiol* 83: 3337–3350, 2000. In a previous study, we combined joint kinematics and electromyograms (EMGs) to examine the change in the phase relationship of two principal leg joints during walking and searching. In this study, we recorded intracellularly from motor neurons in semi-intact behaving animals to examine mechanisms coordinating extension at these leg joints. In particular, we examined the change in the phase of the coxa-trochanter (CTr) and femur-tibia (FT) joint extension during walking and searching. In doing so, we discovered marked similarities in the activity of CTr and FT joint extensor motor neurons at the onset of extension during searching and at the end of stance during walking. The data suggest that the same interneurons may be involved in coordinating the CTr and FT extensor motor neurons during walking and searching. Previous studies in stick insects have suggested that extensor motor neuron activity during the stance phase of walking results from an increase in tonic excitation of the neuron leading to spiking that is periodically interrupted by centrally generated inhibition. However, the CTr and FT extensor motor neuron activity during walking consists of characteristic phasic modulations in motor neuron frequency within each step cycle. The phasic increases and decreases in extensor EMG frequency during stance are associated with kinematic events (i.e., foot set-down and joint cycle transitions) during walking. Sensory feedback associated with these events might be responsible for phasic modulation of the extensor motor neuron frequency. However, our data rule out the possibility that sensory cues resulting from foot set-down are responsible for a decline in CTr extensor activity that is characteristic of the *Blaberus* step cycle. Our data also suggest that both phasic excitation and inhibition contribute to extensor motor neuron activity during the stance phase of walking.

INTRODUCTION

Many motor tasks require coordination of multiple motor pools to execute a behavior. For articulated animals, the pattern of activity and phase relationships of motor neurons acting on muscles at several joints in several legs must be coordinated. Coordination of motor neuron activity typically results from interactions between central influences and peripheral sensory feedback (Angel et al. 1996; Bassler 1993; Brunn 1998; Graham and Bassler 1981; Grillner and Zangger 1979; Hess and Buschges 1999; Robertson et al. 1985). In insects, interneurons have been described that receive and integrate central and afferent input and coordinate activity of motor pools acting at several leg joints (Burrows 1980, 1981; Hisada et al. 1984; Siegler 1985; Wilson and Phillips 1983). However, their contribution to coordination of motor neuron activity has rarely been described in behaving animals (Kitmann et al. 1995; Schmitz et al. 1991). In behaving stick insects, a parallel and distributed network of interneurons orchestrates coordination of multiple joints (Kitmann et al. 1995). The activity of each of these interneurons either supports or opposes movements of ongoing active behaviors (walking, searching, rocking) and postural reflexes (Kitmann et al. 1995).

While distributed neural networks are adaptive for behavior, they present several challenges for understanding inter-joint coordination based on activity of interneurons. First, the output of convergent interneuron pathways impinges onto a relatively small set of motor neurons, yet not all of this information is used to shape motor activity. For example, weak synaptic strengths or presynaptic inhibition resulting from central or afferent influences may lesson the contribution of some interneurons to a particular behavior (Burrows and Matheson 1994; Cattaert et al. 1990, 1992; El Manira et al. 1991; Sauer and Buschges 1994; Sillar and Skorupski 1986; Wolf and Burrows 1995). Therefore one could record activity from interneurons that is consistent with their role in supporting or opposing an ongoing behavior, yet those interneurons may in effect not contribute to shaping ongoing motor neuron activity. Second, in addition to input from interneurons, motor neuron activity producing a behavior results from the integration of direct synaptic inputs from afferents and is dependent on the passive and active membrane properties of the motor neuron itself. These influences on motor neuron activity are separate from those produced by interneurons, are not reflected in recordings made from interneurons, and may have marked effects on coordination of multiple joints.

These potential problems point to the necessity of analyzing neural activity associated with a particular behavior while the animal is performing that behavior. It is technically impractical to use intracellular techniques to examine the activity from a large group of interneurons while an insect performs multiple motor tasks. Nevertheless reasonable progress can be achieved in understanding the neural basis of multi-joint coordination by recording intracellular activity from a sample of motor neurons that act at different joints during ongoing behaviors (Godden and Graham 1984; Robertson and Stein 1988; Wolf 1990). The results of these studies can then be used to generate testable hypotheses regarding the underlying neural organization that orchestrates complex behaviors (Robertson and Stein 1988). In this study, we recorded from two principal leg motor neurons while semi-intact tethered cockroaches walked or searched for a foothold. The activity of these motor neurons results in the extension of either the coxa-trochanter (CTr) or femur-tibia

The costs of publication of this article were defrayed in part by the payment of page charges. The article must therefore be hereby marked "*advertisement*" in accordance with 18 U.S.C. Section 1734 solely to indicate this fact.

(FT) joints. In this paper, we examine synaptic input to these motor neurons to establish criteria for identifying interneurons that may coordinate extension of these joints during walking and searching.

Examination of extensor motor neuron activity during both treadmill (Watson and Ritzmann 1998a) and tethered walking (Tryba and Ritzmann 2000) revealed that there are characteristic intraburst features that include rapid increases and decreases in frequency at particular points during a step cycle. These data suggested that both phasic excitation and inhibition coordinate extensor activity during a rhythmic behavior such as walking. In contrast, data from fictive locomotion recorded from the deafferented ganglia of stick insects (Buschges 1998) and implications from the flexor burst generator model (Pearson 1976) suggest that extensor motor neuron activity is primarily the result of an increase in tonic excitation that is periodically interrupted by rhythmic inhibition that is centrally generated. The characteristic phasic modulation of slow depressor coxa neuron (Ds) and slow extensor tibia neuron (SETi) frequency found in intact walking may result from both central and sensory influences. Active membrane properties that are revealed during intact behaviors (see Ramirez and Pearson 1991) but not necessarily observed during fictive locomotion may also contribute to phasic modulation. To begin to test these hypotheses, we studied whether there are specific kinematic events such as foot touch down and joint cycle transitions that may be associated with characteristic changes in motor neuron firing frequency. We also examined whether we could identify the principal synaptic inputs that are responsible for the characteristic phasic modulation of Ds and SETi activity at the end of stance. Because a similar extensor coordination is observed during searching, we believe that the same interneurons may coordinate activity of Ds and SETi at the end of stance and during searching.

When cockroaches lose ground contact, they switch behaviors from walking to searching (Tryba and Ritzmann 2000). The most prominent differences observed as a result of this switch involved the joint movements associated with swing and stance phases. During walking, flexion at the CTr and FT joints occurred during swing phase, whereas when the animal searches, these joints extend during the aerial phase. In both of these behaviors, leg protraction involves complex actions of the body-coxa joint that have yet to be examined in detail. However we did find consistent differences in movements at the more distal joints of the middle legs when the animal switched from walking to searching. During walking, the CTr extension precedes extension of the FT joint, whereas during searching, the onset of CTr extension was delayed relative to the FT extension. Joint movements that occurred during searching were coincident with a characteristic electromyographic (EMG) pattern recorded from CTr extensor (Ds) and FT extensor (SETi) motor neurons that included high-frequency SETi activity prior to the onset of Ds activity (Tryba and Ritzmann 2000). A high-frequency burst in SETi coupled with a decrease in Ds activity is also seen at the end of stance phase of walking. However, the kinematics at the FT joint are different in the two behaviors. We hypothesize that the pattern of high-frequency SETi activity in conjunction with the cessation of Ds activity either at extension onset during searching or at the end of stance during walking involves excitation of SETi and inhibition of Ds. We further propose that the same interneuron(s) coordinate Ds and SETi activity at those times. In this study, we recorded intracellularly from Ds and SETi during tethered walking and searching to test whether we can account for the phase relationship of the CTr and FT joints at the end of the stance phase and the onset of searching.

METHODS

Animals

Adult male death-head cockroaches (*Blaberus discoidalis*) were used in all experiments. Cockroaches were raised in our own colony descended from 250 adult animals generously provided by Dr. Larry L. Keeley of Texas A & M University. Cockroaches were housed in 20 l plastic buckets, half filled with aspen shavings, and were held at 27°C in a 12 h light:12 h dark circadian cycle. A commercial dry chicken starter and water were provided ad libitum. Only intact, undamaged cockroaches were used.

Preparation of semi-intact tethered animals for intracellular recording

To gain access to the ganglia of interest, we needed to remove the dorsal cuticle of the animal, eviscerate the animal, and stabilize the mesothoracic ganglion. We also needed to stabilize the dorsal cuticle to keep the remaining cuticle from tearing while the animal engaged in searching or walking behaviors. Stabilization of the dorsal cuticle was done by gluing a U-shaped piece of aluminum to the dorsal cuticle with cyanoacrylate glue. The aluminum was cut into a U-shape from a soda-pop can pull-tab and glued to the dorsal cuticle while the animal was under CO_2 anesthesia (Fig. 1, *A* and *B*). The top of the U abutted the posterior edge of the animal's pronotum. A U-shaped insect pin (No. 2) was glued onto the pronotum cuticle and onto part of the pull-tab. The insect pin was bent so as to form-fit the shape of the pronotum. The insect pin and pull tab were glued end to end such that they formed an O shape on the dorsal cuticle to stabilize it (Fig. 1, *A* and *B*). Next, EMG electrodes were implanted to record from the mesothoracic depressor trochanteris muscle and extensor tibia muscle as described extensively by Watson and Ritzmann (1998a) and in the companion paper (Tryba and Ritzmann 2000). The coxal depressor muscle is innervated by one slow excitatory motor neuron (Ds), one fast excitatory motor neuron (Df) and three inhibitory motor neurons (Pearson and Iles 1971). Excitatory innervation of the extensor tibia muscle includes slow and fast extensor tibia motor neurons (SETi and FETi).

The animal was pinned to a cork platform and the dorsal cuticle circumscribed by the pull tab and pin was removed. Next, the animal was eviscerated to expose the three thoracic ganglia. The thoracic body cavity was rinsed and filled with saline solution. Just posterior to each of the ganglia, above nerve 5 roots, there is some overlying cuticle that was removed from each of the thoracic ganglia. This procedure allowed the ganglia to move more independently of the remaining cuticle. The animal was tethered using two insect pins stuck through its pronotum on either side of its head as described in the companion paper (Tryba and Ritzmann 2000) (Fig. 1, *A* and *B*). The tethered animal was then placed on the glass substrate made slick with microtome oil (Lipshaw Manufacturing, microtome oil No. 288). The tether was the same as in our previous study (Tryba and Ritzmann 2000) with the exception that the pins were glued to the pronotum where they passed along the underside of the pronotum and also where they passed through the pronotum. Gluing the pins to the pronotum provided a more rigid tethering of the animal so that intracellular recordings could be made. Next the mesothoracic (T2) ganglion was stabilized using a custom built metal spoon-shaped platform that was form-fitted to the ventral surface of the T2 ganglion. The ganglion was supported by the platform and further stabilized by a custom built metal ring that was compressed onto the dorsal surface

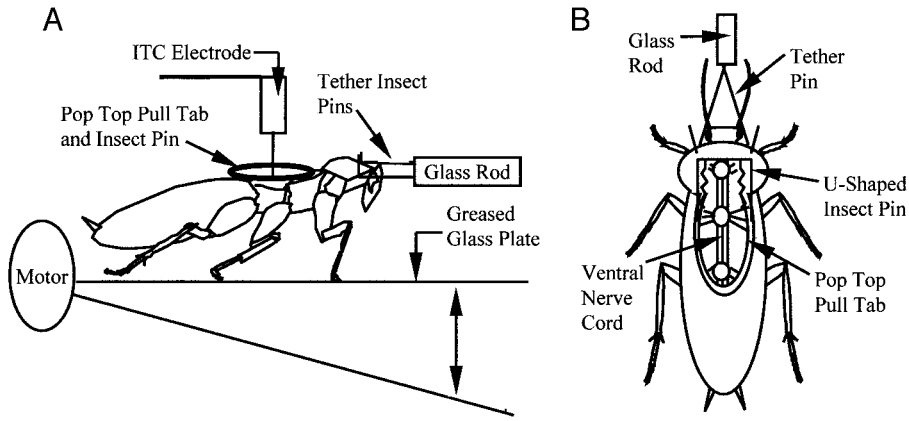

FIG. 1. *A*: semi-intact, tethered preparation set-up for simultaneous electromyography (EMG, wires not shown), high-speed videography, and intracellular recording (ITC electrode) during walking and searching. Illustration of a cockroach tethered on a glass plate made slick with microtome oil. Pitching the glass plate away (double-headed arrow) from the anterior of the animal results in the animal switching from walking to searching movements with its front and middle legs. A portion of a pop-top pull-tab was glued onto the dorsal cuticle along with a bent insect pin. Animals were tethered by 2 insect pins poked through their pronotum. The other end of the pins were attached to a glass rod that was then held by a micromanipulator (not shown). *B*: dorsal view illustrating the arrangement of the U-shaped piece of pop-top pull-tab and U-shaped insect pin. The dorsal cuticle circumscribed by the pop-top pull-tab and bent insect pin was removed and the animal eviscerated to gain access to the mesothoracic ganglion.

of the ganglion to sandwich it between the ventral platform and dorsal compression ring (Wolf and Pearson 1987).

Walking was induced by gently tapping on the dorsal abdomen with a wooden dowel. A walking animal was induced to search for a foothold by pitching the glass substrate away from the animals' anterior as described previously (Tryba and Ritzmann 2000). We refer to this preparation as a semi-intact tethered preparation.

Blaberus saline

The saline solution used for both dissection and intracellular recording consisted of (in mM) 140.0 NaCl, 10.0 KCl, 9.0 CaCl, and 5.0 MgCl in distilled water. The pH was buffered to 7.2 with 3-[N-morpholino]propanesulfonic acid (Sigma) and sodium salt.

Intracellular recordings

Intracellular recordings were made from the Ds, FETi, and SETi motor neurons. Recordings were made from the neuropile of the second thoracic ganglia (T2) while the animal engaged in searching or walking behaviors. We also recorded from interneurons that had processes in the posterior quadrant of the T2 ganglia, medial to nerve 5 roots. Intracellular microelectrodes were pulled from single tube capillary glass (World Precision Instruments). Their tips were filled with a solution of 4% Lucifer yellow CH (Molecular Probes) in 0.1 M lithium acetate (Sigma). The remainder of the electrode was backfilled with 1.0 M lithium acetate. Resistances consistently ranged from 60 to 80 MΩ. To facilitate penetration of the sheath surrounding the ganglia with the recording electrode, we applied a small piece of cotton soaked with Protease Type XIV (1.0 mg/ml; Sigma) to the ganglia and allowed the protease access to the sheath for 3×5 min. The cotton was removed and the thoracic cavity was rinsed (4 times) and then filled with *Blaberus* saline. The dorsal neurilium was then penetrated with a recording electrode. The electrode was gradually advanced into the neuropile, and capacitance ringing of the electrode tip resulted in motor neuron impalement in the neurite region, indicated by synaptic activity. Records were stored on a VHS Vetter recording system (equipped with an A/D converter) and played back for acquisition and analysis using Axotape recording software (Axon Instruments).

Identification of motor neurons and interneurons

The microelectrodes were filled with Lucifer yellow in the hope of using morphological cues for positive identification of neurons. However, we were unsuccessful at injecting dye into the neurons that we recorded from. Instead motor neuron identification was made by injecting depolarizing and hyperpolarizing current of sufficient magnitude to increase and null the corresponding EMG activity. The action potential activity recorded intracellularly from each motor neuron also matched one for one with recorded muscle potentials (EMGs).

A demonstration of direct connectivity between interneurons and a motor neuron requires simultaneous intracellular recordings from both cells. However, because intracellular recordings in the tethered preparation could only be maintained for short periods, we considered paired intracellular experiments to be unreasonable. We were able to provide indirect evidence that a particular interneuron influences the activity of Ds and/or SETi (directly or indirectly) by injecting hyperpolarizing or depolarizing current into the interneuron and noting changes in motor neuron activity. Of course, the recorded interneurons could also influence the activity of additional motor neurons and/or interneurons that were not monitored. The interneurons were classified as nonspiking interneurons if action potentials were not elicited at any level of depolarization tested despite changes in motor neuron activity.

When recording from motor neurons and interneurons during leg movements, current injections were performed before and after the animals' behavior was examined to ensure the recording electrode remained in the same cell throughout the recording. To control for movement artifacts in the intracellular records taken during behavior, the electrode was removed from the cell, and the animal was again induced to perform walking and searching movements with the electrode just outside the cell. Movement artifact did not appear to contribute to the reported voltage deflections.

Joint kinematics

True joint angles were calculated for the T_2 CTr and FT joints during tethered walking. Methods used to collect and calculate the joint kinematic data were described extensively by Watson and Ritzmann (1998a) and in the companion paper (Tryba and Ritzmann 2000). To capture the leg movements, we used a high-speed digital video system (Redlake HS500) aimed at the lateral projection of the tethered cockroach. A mirror angled at 45° beneath the glass substrate allowed us to capture both a ventral and lateral view of the animal (see

Tryba and Ritzmann 2000). To obtain a very precise ventral view, we placed the angled mirror as close as possible to the underside of the glass plate the tethered animal walked on. Placing the mirror up against the glass plate prevented us from pitching the glass plate away from the anterior of the animal to induce the animal to switch to searching (see Tryba and Ritzmann 2000). Therefore the combined kinematic and intracellular data reported here were collected only during walking.

RESULTS

T2 tethered semi-intact walking

RELATIONSHIP OF T2 DS AND SETi ACTIVITY TO JOINT KINEMATICS. To establish whether or not the semi-intact tethered preparation yields biologically relevant walking data, we compared the relationship between motor neuron activity and joint kinematics for intact tethered, semi-intact tethered, and freely walking

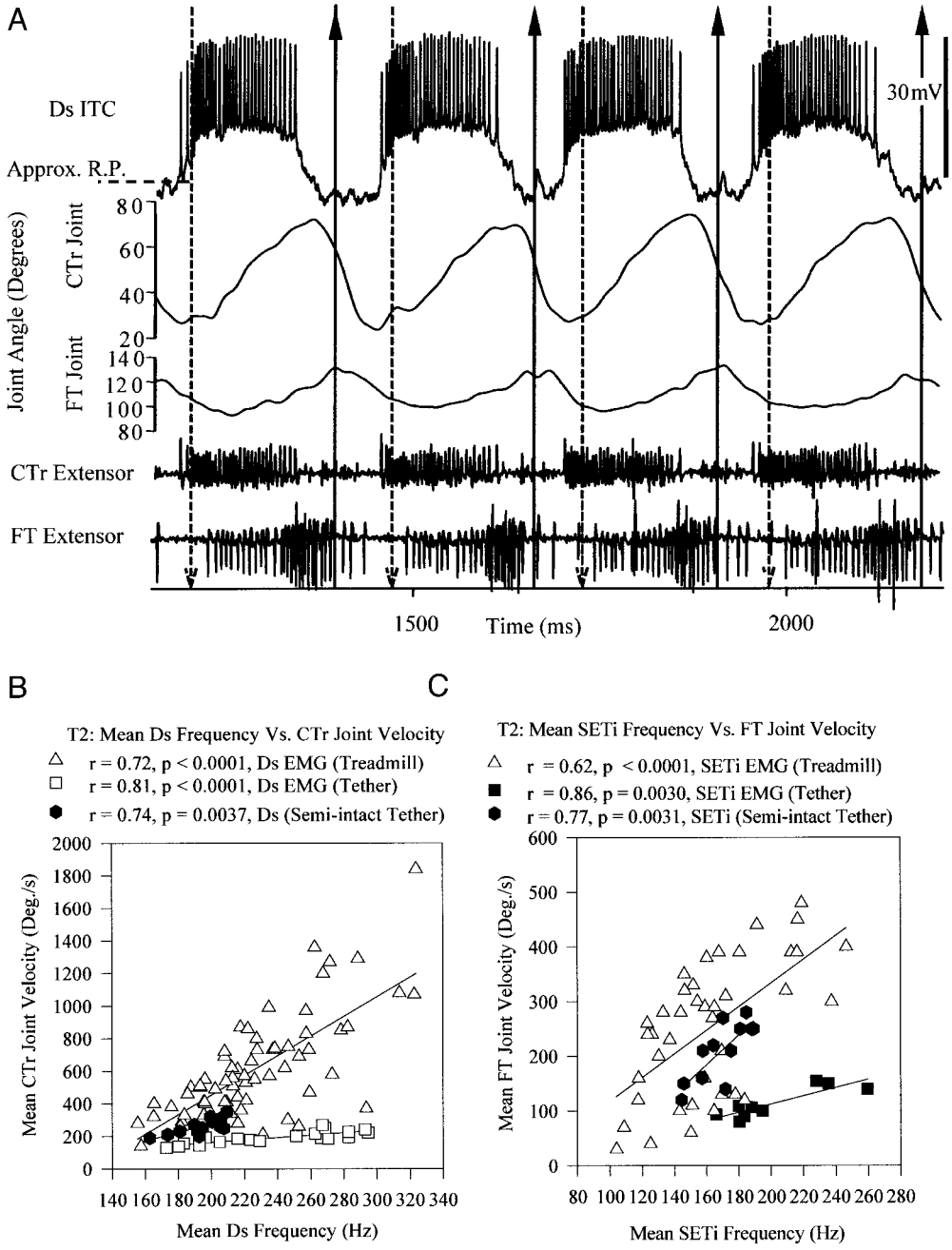

FIG. 2. *A*: intracellular recording from slow depressor coxa neuron (Ds; Ds ITC, *top*, scale bar: 30 mV), coxa trochanter (CTr) and femur tibia (FT) true joint angles (*middle 2 traces*), and CTr and FT extensor EMGs (*bottom 2 traces*) during tripod walking. Record from a semi-intact tethered animal walking on a glass plate. Upward vertical solid arrows indicate when the foot (tarsus) lifted off the glass plate, while downward vertical dashed arrows indicate foot set-down. Horizontal dashed line (*left* of Ds ITC record) marks the approximate resting potential. Ds activity is smaller and fast depressor coxa neuron (Df) activity is larger amplitude potentials in the CTr extensor record. Slow extensor tibia neuron (SETi) activity and fast depressor tibia neuron (FETi) activity are smaller and larger amplitude potentials (respectively) in the FT extensor record (see also Tryba and Ritzmann 2000). The *y*-axis scale is in reference to the original recording and does not begin at 0. *B*: plot of the mean Ds frequency (Hertz) vs. mean CTr joint angular velocity (deg/s) for T2 leg during treadmill walking (open triangles), intact (open squares), and semi-intact (closed hexagon) tethered walking. *C*: plot of the mean SETi frequency (Hertz) vs. mean FT joint angular velocity (deg/s) for T2 leg during treadmill walking, intact, and semi-intact tethered walking. Symbols are as in *B*.

cockroaches. Motor neuron frequency markedly influences the rate of muscle contraction and in turn joint angular velocity during horizontal treadmill walking (Watson and Ritzmann 1998a) and tethered walking (Tryba and Ritzmann 2000). Accordingly, during walking there is a linear relationship between mean frequency of slow motor neuron activity and mean joint angular velocity (Tryba and Ritzmann 2000; Watson and Ritzmann 1998a). A similar relationship should exist between the motor neuron activity and joint velocity for semi-intact tethered cockroaches during walking if they walk in a reasonably normal way. To test this, we plotted mean Ds and SETi frequency and mean CTr and FT joint velocity using EMG data obtained from a single semi-intact preparation during an intracellular recording of Ds (Fig. 2, *A–C*). In that case, CTr data shown include 13 CTr joint extensions, while FT data represent 12 joint extensions (Fig. 2*B*). We compared the relationship between motor neuron activity and leg kinematics during: walking on a horizontal treadmill (Watson and Ritzmann 1998a), intact tethered walking (Tryba and Ritzmann 2000), and semi-intact tethered walking during an intracellular recording of Ds. During some step cycles in the semi-intact walking data, fast motor neurons were recruited (Fig. 2*A*). Of the 12 SETi bursts examined, six steps included two FETi potentials, while the remaining six had one FETi potential per burst. In contrast, only two of the Ds bursts included fast potentials with each of these bursts having one Df potential. As with other preparations, the mean CTr or FT joint extension velocity of the semi-intact preparation was correlated with the related mean slow (Ds or SETi) motor neuron activity ($r = 0.74$ and $r = 0.77$, respectively; Fig. 2, *B* and *C*). A given mean extensor motor neuron frequency resulted in a lower mean CTr or FT joint velocity than during treadmill walking. However, it was higher than the intact tethered walking preparations (Fig. 2, *B* and *C*). We propose possible reasons for these differences in DISCUSSION.

INTRACELLULAR RECORDING OF T2 DS DURING TETHERED WALKING. Having established that the relationship between semi-intact tethered walking motor neuron activity and joint kinematics is linear, as is the case for freely walking animals, we then investigated mechanisms patterning extensor motor neuron activity during walking. We examined the hypothesis that the pattern of activity for walking found in extensor motor neurons results primarily from an increase in tonic depolarization that is periodically interrupted by inhibition (see Buschges 1998). We marked on the intracellular records the approximate resting potential of Ds by extending a straight line across the baseline of tonic activity recorded when the animal was not moving its legs (i.e., prior to walking) to the area of the record that included walking (Fig. 2*A*). During bursts of activity associated with walking, the membrane potential of Ds was depolarized above resting conditions. Data collected from Ds recordings represent 58 walking step cycles from four animals.

To further establish that Ds is depolarized during walking, we compared the mean action potential amplitude during walking with that when the animal was not moving its legs (prior to or after a bout of walking). There was a 33.2% decrease in mean Ds action potential amplitude during walking [19.85 ± 0.95 (SD) mV] compared with activity before or after a walking bout [29.73 ± 0.75 (SD) mV] when the animal was not moving its legs ($n = 2$ animals, 142 action potentials measured during walking, 100 action potential amplitudes measured before or after walking). The action potential amplitude was measured before and after walking in our analysis to ensure that the changes in action potential amplitude were not due to changes in the quality of the recording.

During walking, Ds undergoes a rapid depolarization prior to tarsus touchdown or CTr extension (Fig. 2*A*). The rapid initial depolarization of Ds is followed by a period of high-frequency Ds activity characteristic of the first 10–15% of the burst (Watson and Ritzmann 1998a). The Ds frequency declines after the initial high-frequency period, but the membrane potential remains at a depolarized level throughout the burst (Fig. 2*A*). The decline in mean Ds spike amplitude during walking can be attributed to a relatively stable depolarization of Ds during bursting (Fig. 2*A*). The mean amplitude of this maintained depolarization as measured between spikes was 11.78 ± 0.98 mV ($n = 70$ observations, 1 animal) above the perceived resting potential (−55 mV). The decrease in spike amplitude is consistent with a decrease in driving force on the cation(s) responsible for depolarization during Ds action potentials (i.e., Na^+, Ca^{2+}, or both). During a Ds burst, we could occasionally observe excitatory postsynaptic potentials (EPSPs) leading to action potentials (Fig. 3*A*). At the end of the burst, inhibitory postsynaptic potentials (IPSPs) are evident as the membrane potential is rapidly repolarized (Fig. 3*B*, downward arrows). Thus inhibitory input apparently contributes to burst termination and interburst intervals of Ds activity (see also Buschges 1998; Godden and Graham 1984) (Fig. 3*C*). In support of this hypothesis, between bursts Ds was hyperpolarized by a maximum of 4.73 ± 1.05 mV ($n = 12$ observations, $n = 1$ animal).

INTRACELLULAR RECORDINGS FROM NONSPIKING INTERNEURONS DURING WALKING. Having found that both inhibition and excitation pattern Ds activity, we then searched for evidence of interneurons that could provide this type of synaptic input to Ds during walking. We recorded from two nonspiking interneurons whose activity is consistent with influencing Ds activity during walking. When the animal is not moving its legs, injection of depolarizing current into one of these nonspiking interneurons (NSI-A) results in a decrease in Ds EMG activity, while hyperpolarization increases Ds activity (Fig. 4, *A* and *B*).

During walking, NSI-A is depolarized beginning about the middle of the Ds burst ($n = 33$ steps, $n = 1$ animal). The rate of depolarization of NSI-A increases just after Ds burst termination (Fig. 4*C*). It then begins to repolarize roughly halfway through the Ds interburst period (Fig. 4*C*). Hyperpolarizing current injected into NSI-A at an intensity sufficient to result in Ds action potentials when the animal was not walking did not increase Ds burst duration during walking (Fig. 4*D*; $n = 3$ trials).

In contrast to NSI-A, NSI-B provides excitatory drive to Ds in nonwalking animals (Fig. 5*A*). That is, Ds activity increases during depolarization of NSI-B when the animal is not moving its legs (Fig. 5*A*, $n = 8$ trials, $n = 1$ animal). During walking, NSI-B begins to depolarize just prior to the onset of the Ds burst (Fig. 5*B*; $n = 1$ animal, $n = 56$ steps). It then repolarizes just before the Ds burst terminates (Fig. 5*B*). Current injection resulting in hyperpolarization (2 nA) or depolarization (10 nA) of NSI-B during walking shortened ($n = 2$ of 5 trials) and prolonged ($n = 3$ of 3 trials) Ds burst duration (Fig. 5, *C* and *D*). The three trials where hyperpolarization failed to shorten

the Ds burst duration involved current injection in the first half of the Ds burst, whereas effective stimuli occurred in the second half of the burst. When Ds burst duration was altered following current injection into NSI–B when the animal walked, the burst duration of SETi was altered in parallel (n = 5 trials) even though SETi activity was not affected following current injection into NSI-B when the animal was not walking (Fig. 5, *C* and *D*).

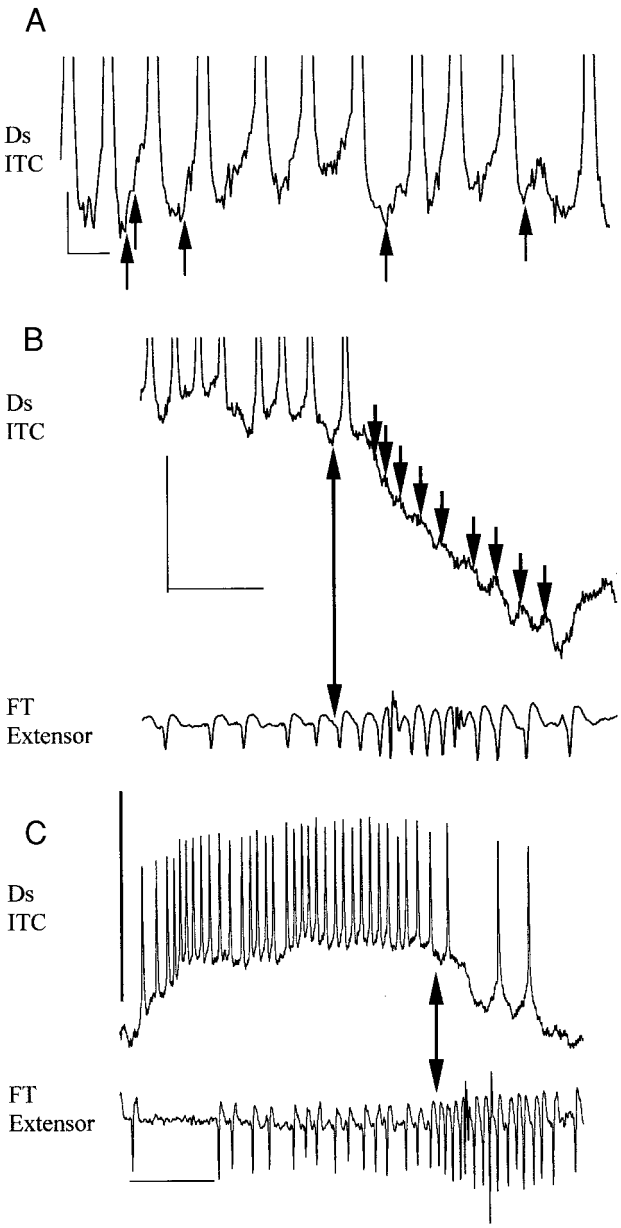

FIG. 3. *A*: expanded portion of Ds intracellular (Ds ITC) burst record during semi-intact tethered walking. Note that the beginning and end of the burst are not shown. Spikes are truncated in favor of showing greater detail at the baseline. Upward arrows indicate excitatory postsynaptic potentials (EPSPs). Scale bar: 10 ms, 2 mV. *B*: Ds intracellular record (Ds ITC) and FT extensor EMG (*bottom*) during semi-intact tethered walking. Beginning of the Ds burst and FT extensor burst are not shown. Downward arrows indicate inhibitory postsynaptic potentials (IPSPs); double-headed arrow marks onset of high-frequency SETi activity. Scale bar: 20 ms, 10 mV. *C*: intracellular record of Ds burst (Ds ITC) and FT extensor EMG burst (*bottom*) during semi-intact tethered walking. Double-headed arrow as in *B*. Vertical bar: 30 mV, horizontal scale bar: 50 ms.

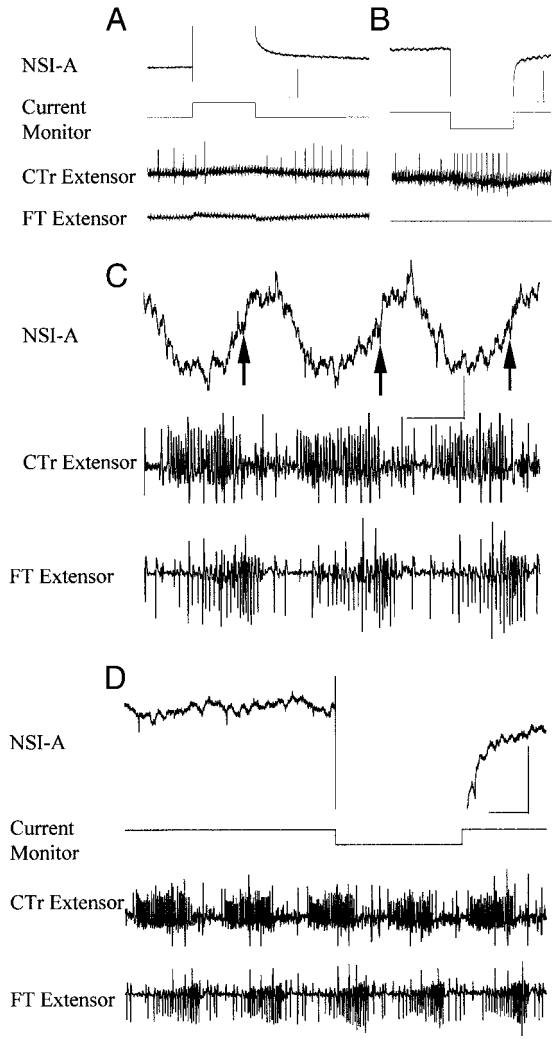

FIG. 4. *A*: intracellular recording from nonspiking interneuron "A" (NSI-A) during depolarizing current injection (1 nA). The animal was not moving its legs during current injection. Bridge is unbalanced. Also shown are CTr and FT extensor EMGs (*bottom 2 traces*). Depolarization of NSI-A resulted in a decline in slow CTr extensor activity. Scale bar: 100 ms, 40 mV. *B*: hyperpolarization of NSI-A resulted in an increase in slow CTr extensor activity when the animal was not moving its legs. Bridge is unbalanced. Labels as in *A*. Scale bar: 100 ms, 20 mV. *C*: intracellular recording of NSI-A and simultaneous CTr and FT extensor EMGs during semi-intact tethered walking. Upward arrows indicate rapid depolarization of NSI-A associated with Ds burst termination. Labels as in *A*. Scale bar: 100 ms, 10 mV. *D*: hyperpolarizing current injection (5 nA) into NSI-A during semi-intact tethered walking did not appear to alter CTr slow extensor burst duration. Labels as in *A*. Scale bar: 100 ms, 25 mV.

RELATIONSHIP OF Ds ACTIVITY TO T2 FOOTFALL AND CTr JOINT ANGLE. Phasic modulation of motor-neuron frequency during walking may result in part from central or sensory influences and in part from active membrane properties. We examined the relationship among Ds activity, footfall, and CTr joint angle to determine whether sensory feedback during specific kinematic events such as foot set-down and movement through a joint angle is likely to trigger phasic modulation of motor extensor activity. During walking, Ds motor neuron activity begins before foot set-down with high-frequency activity within the first 10% of the burst (Fig. 2*C*) (see also Watson and Ritzmann 1998a).

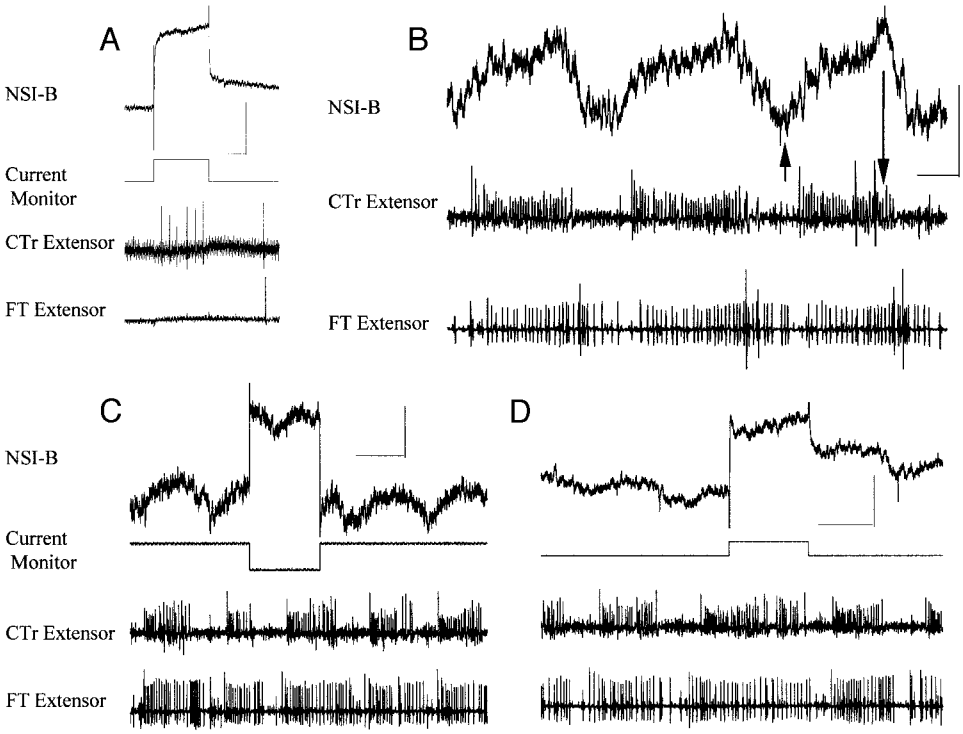

FIG. 5. *A*: intracellular recording from nonspiking interneuron "B" (NSI-B) during depolarizing current injection (1 nA). The animal was not moving its legs during current injection. CTr and FT extensor EMGs are also shown (*bottom 2 traces*). Depolarization of NSI-B resulted in an increase in slow CTr extensor (Ds) activity. Scale bar: 100 ms, 20 mV. *B*: intracellular record of NSI-B activity (*top*), CTr and FT extensor EMGs (*bottom 2 traces*) during semi-intact tethered walking. Upward arrow indicates onset of NSI-B depolarization; downward arrow indicates where NSI-B begins to repolarize. Scale bar: 100 ms, 5 mV. *C*: hyperpolarizing current injection (10 nA) during semi-intact tethered walking resulted in a decrease in CTr extensor (Ds) and FT extensor (SETi) burst duration. Scale bar: 200 ms, 5 mV. *D*: depolarizing current injection (5 nA) during semi-intact tethered walking resulted in an increase in CTr extensor (Ds) and FT extensor (SETi) burst duration. Scale bar: 200 ms, 5 mV.

Thereafter there is a decline from peak instantaneous frequency near foot set-down ($n = 2$ animals, 18 steps) (Watson and Ritzmann 1998a). Several candidates exist for sensory cues at the time of foot set-down that may influence this decline in Ds activity. Tactile receptors in the foot or strain detectors (i.e., campaniform sensilla) in the leg cuticle could detect foot contact directly. Alternatively, joint angle detectors such as the chordotonal organs could produce the decline when they detected a particular joint angle or joint velocity. Still another possibility is that the decline is centrally patterned.

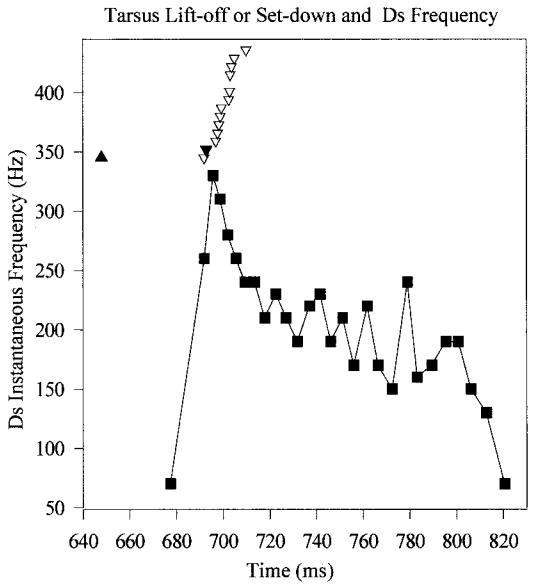

FIG. 6. Instantaneous frequency plot of Ds activity recorded intracellularly during semi-intact tethered tripod walking. Upward solid triangle indicates when the foot (tarsus) lifted off the substrate. Downward solid triangle indicates foot set-down. Foot set-down times from 12 other step cycles (▽) are plotted with their occurrence normalized relative to the peak instantaneous Ds frequency. Triangle *y*-axis placement is arbitrary.

To begin to test these possibilities, we plotted the instantaneous frequency of Ds activity together with the times of foot set-down. In 16 of 18 step cycles (88.89%), the decline in instantaneous Ds frequency occurred prior to foot set-down and in the remaining 2 instances, the decline happened after foot set-down ($n = 2$ animals). The instantaneous frequency of one Ds burst is plotted along with the time of foot lift off and set-down that occurred during that step cycle (1 animal; Fig. 6). Also shown are the times that foot set-down occurred during 12 other steps in the walking sequence relative to the peak Ds frequency in their respective cycles (Fig. 6). In most of these cycles (61.5%), foot set-down occurred after the peak Ds frequency. These data indicate that the decline in Ds frequency cannot be due to feedback from afferents detecting foot set-down or cuticular strain.

The decline in instantaneous frequency of Ds occurred just prior to onset of CTr extension during the swing to stance transition (Tryba and Ritzmann 2000). It is possible that joint angle detectors might be involved in initiating this characteristic decline in Ds activity. To examine this problem, we measured the CTr joint angle at the time of peak Ds instantaneous frequency. We chose this point in the Ds records as it occurred prior to the decline in instantaneous frequency and because it could be found consistently from step cycle to step cycle. The CTr joint angle at the time of the peak instantaneous Ds frequency was consistently near $31.5 \pm 3.2°$ ($n = 1$ animal, 9 cycles). The range of joint angles (maximum-minimum values) was 10.6° or 21.6% of the mean CTr joint excursion of 49.1°. Watson and Ritzmann (1998a) also found that the Ds high-frequency period ends at $24.3 \pm 5.0°$ in T2 legs when cockroaches walked on a treadmill. These data suggest the decline in Ds frequency may be due to feedback from joint angle detectors.

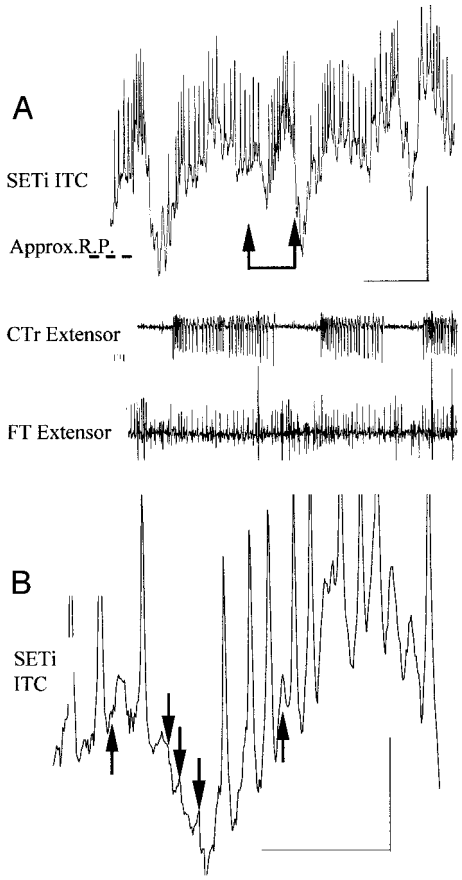

FIG. 7. *A*: simultaneous intracellular recording from mesothoracic leg SETi (SETi ITC, *top*, scale bar: 200 ms, 10 mV) and CTr and FT extensor EMGs during tripod walking (*bottom 2 traces*). Record from a semi-intact tethered animal walking on a glass plate. Approximate resting potential is shown as dashed horizontal line (Approx. R. P.). Bracketed upward arrows connected by a line indicate portion of record expanded in *B*. *B*: expanded record of SETi ITC activity during tethered walking. Upward arrows indicate EPSPs, downward arrows indicate IPSPs. Scale bar: 100 ms, 2 mV.

Intracellular recording of SETi during tethered walking

As was the case for Ds, the frequency of SETi activity changes in a characteristic way throughout a burst when the animal walks. Thus we examined whether or not SETi also receives excitatory synaptic input that may contribute to modulation of its firing frequency during walking. At the start of a SETi burst, there is low-frequency activity that is typically followed by high-frequency activity beginning during the last 70% of the burst cycle (Fig. 7*A*) (Tryba and Ritzmann 2000; Watson and Ritzmann 1998a). As is the case for Ds when the animal walks, the membrane potential of SETi during a burst is also depolarized relative to the approximate resting potential extrapolated from the baseline prior to a bout of walking (Fig. 7*A*). Quantitative data from the SETi represent intracellular data recorded for 22 walking cycles from two animals. EPSPs could be observed to precede some of the SETi action potentials (Fig. 7*B*).

Coordination of CTr and FT extensor motor neurons at the end of stance phase of walking

Having examined some of the mechanisms coordinating either Ds or SETi activity during walking, we then investigated how the activity of both of these motor neurons might be orchestrated together. Throughout much of the stance phase of walking, Ds and SETi are simultaneously active (Figs. 2*C* and 8*A*) (Watson and Ritzmann 1998a). The end of stance phase involves inhibition of Ds at about the same time high-frequency SETi activity begins (Figs. 2*A* and 3, *B* and *C*). The high-frequency SETi activity results from rapid depolarization of SETi at the end of stance (Figs. 2 and 7*A*).

There are several neural mechanisms that could account for the nearly simultaneous onset of Ds inhibition and high-frequency SETi activity. One way to achieve this coordinated activity would be to have SETi directly inhibit Ds. This hypothesis can be eliminated, as there did not appear to be a 1 for 1 correlation between SETi spikes and IPSPs in Ds (Fig. 3*B*).

Alternatively, one or more interneurons could project to both motor neurons where they inhibit Ds and excite SETi. The most direct way to test for this possibility would be to record intracellularly from Ds and SETi simultaneously. However, dual recordings in a tethered preparation during walking would be difficult to achieve. Instead, we evaluated the correlation between the onset of the SETi high-frequency burst and the onset of Ds inhibition. To get a reasonable evaluation of the timing of these events, two individuals visually inspected the SETi records of one animal and independently marked on the records where they perceived there to be a clear increase in SETi frequency. In 2 of 13 bursts examined, there were differences in the perceived onset of high-frequency SETi activity, and these data were not used in the analysis. Next, the time of the last Ds spike was plotted relative to the onset time of SETi high-frequency activity (Fig. 9*A*). In 3 of the 11 Ds bursts, the last spike was 2 ms before the onset of high-frequency SETi activity. In five cases, the last Ds action potential was within 10 ms after the high-frequency SETi activity began and in the remaining three instances, it was 48–56 ms after the start of the rapid SETi firing (Fig. 9*A*). Even when the Ds activity continued, the onset of high-frequency SETi was accompanied by a rapid decline in Ds frequency (Fig. 3*C*). Rapid hyperpolarization of Ds also occurred either

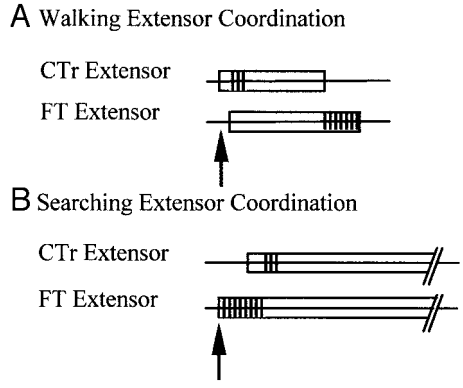

FIG. 8. *A*: summary of mesothoracic (T2) leg walking CTr and FT slow motor-neuron extensor EMG coordination. ↑, onset of a walking extension cycle. Low-frequency Ds and SETi activity is indicated by an open box; high-frequency activity is represented by vertical lines within the open box. *B*: searching CTr and FT slow extensor EMG coordination. Upward arrow indicates approximate search extension onset. Low- and high-frequency activity is represented as in *A*. Termination of low-frequency activity is not indicated as tonic activity continued beyond slanted parallel lines. Data used to make this figure are shown in Fig. 3, *B* and *C*, of Tryba and Ritzmann (2000).

concurrently or shortly following the onset of high-frequency SETi activity (Fig. 3, *B* and *C*).

As the high-frequency phase of SETi activity typically extends to the end of the burst, it is most often seen as a component of a continuous burst (see Watson and Ritzmann 1998a) (Fig. 9*B*). However, in two animals, we found three instances where the high-frequency SETi activity occurred prior to or following the termination of low-frequency SETi activity (Figs. 7*A* and 9, *C* and *D*). In one case, the high-frequency activity occurred as a result of depolarization after the membrane was repolarized following low-frequency SETi activity (Fig. 9*C*). In that case, low-frequency activity in CTr and FT extensor motor neurons terminated simultaneously (Fig. 9*C*). When the high-frequency SETi activity occurred prior to termination of low-frequency Ds and SETi activity (Fig. 9*D*), Ds activity ceased for approximately the same duration as the high-frequency SETi burst, then Ds activity resumed following termination of that event (Fig. 9*D*). In another instance where SETi high-frequency activity began following SETi low-frequency activity, as was the case for Ds, IPSPs contribute to membrane repolarization following low-frequency activity in SETi (Fig. 7*B*).

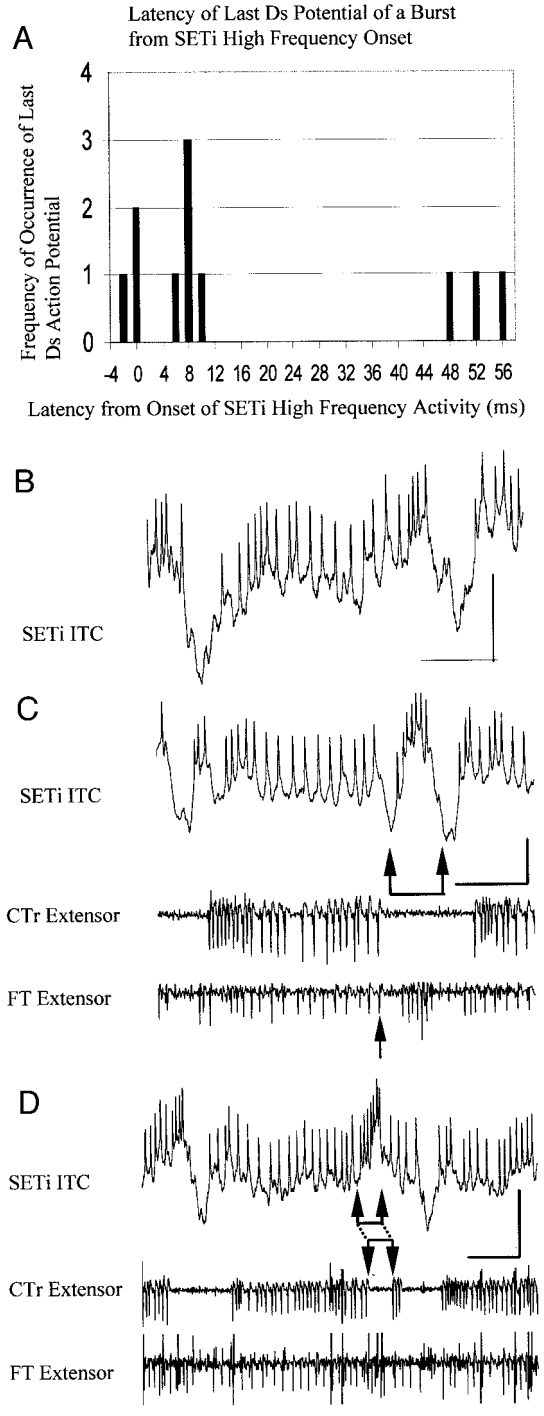

FIG. 9. *A*: histogram showing the latency of the last Ds action potential of a Ds burst relative to the onset of SETi high-frequency EMG activity. *B*: intracellular recording of mesothoracic SETi activity (SETi ITC) during semi-intact tethered walking. Note that SETi begins firing at a low frequency and fires at a high frequency toward the end of the burst. Scale bar: 100 ms, 10 mV. *C*: intracellular recording of SETi activity (SETi ITC) combined with CTr and FT extensor EMGs during semi-intact tethered walking. Bracket area (upward arrows connected by line) shows high-frequency SETi activity can occur after low-frequency activity associated with stance phase. Upward arrow beneath the FT extensor trace marks simultaneous termination of low frequency Ds and SETi activity. Scale bar: 10 ms, 6 mV. *D*: intracellular recording of SETi activity (SETi ITC) combined with CTr and FT extensor EMGs during semi-intact tethered walking. Bracket area (upward arrows connected by line and reflected) shows high-frequency SETi activity can occur prior to termination of low-frequency SETi and Ds activity associated with stance phase. Note that low-frequency Ds activity is interrupted for the duration of SETi high-frequency activity. Scale bar: 10 ms, 10 mV.

It is possible that the cessation of Ds activity and onset of SETi high frequency is due to sensory feedback from joint angle receptors. If that is the case, there should be a consistent relationship between the CTr and/or FT joint angle(s) and onset of the high-frequency SETi activity. We tested this hypothesis by measuring the CTr and FT joint angles at the onset of high-frequency SETi activity. The mean CTr and FT joint angles at that time were 66.3 ± 4.9° and 108.3 ± 3.9° with a range (maximum-minimum values) of 15.8° for CTr and 13.9° for FT (n = 1 animal, 11 cycles). Watson and Ritzmann (1998a) found that the mean T2 FT and CTr excursions during treadmill walking were 26.0° and 43.9°, respectively. Therefore although the standard deviation is relatively small, the range in FT joint angles measured at onset of high-frequency SETi activity during semi-intact tethered walking is actually quite high (60.8% of the total FT excursion during walking). These data suggest that joint angle detectors do not directly cue the onset of these events.

Semi-intact tethered T2 leg searching

INTRACELLULAR ANALYSIS OF Ds ONSET DELAY. Having examined how Ds and SETi are coordinated during walking, we then investigated how these motor neurons are coordinated during searching. As with walking, in describing searching, we will focus first on the pattern of Ds activity, followed by the pattern of SETi activity and finally examine how both of these motor neurons may be coordinated during searching.

Combined joint kinematics and EMGs recorded while cockroaches engaged in T2 leg movements established that there was a delay in the onset of Ds activity relative to SETi during searching versus walking (Fig. 8, *A* and *B*) (Tryba and Ritzmann 2000). Accordingly, the FT joint extends before the CTr joint during searching, whereas during walking CTr extension precedes that of the FT joint (Tryba and Ritzmann 2000).

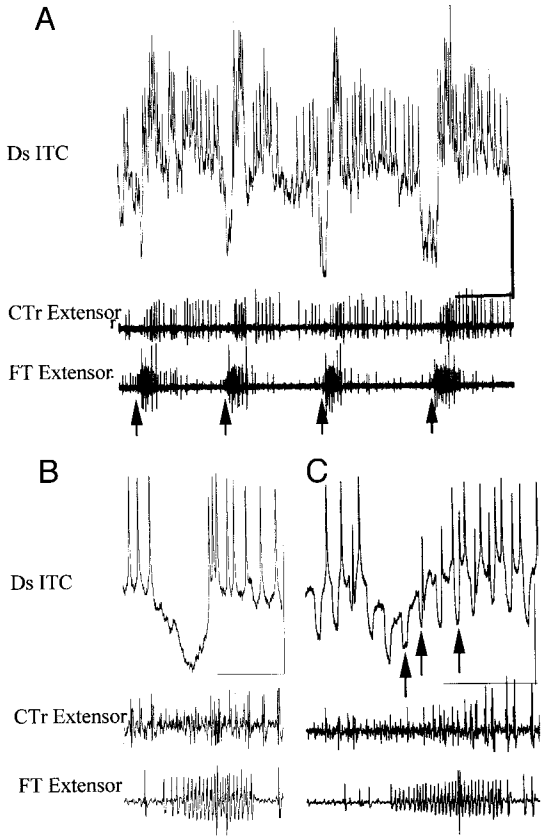

FIG. 10. *A*: intracellular record from Ds (Ds ITC, *top*, scale bar: 500 ms, 15 mV), and CTr and FT extensor EMGs during semi-intact tethered searching. ↑, the approximate start of high-frequency SETi activity. Ds is inhibited just prior to and at the onset of high-frequency SETi activity. *B*: expanded Ds intracellular record during tethered searching showing Ds inhibition at the onset of the searching extension cycle. *C*: constant amplitude (0.25 nA) hyperpolarizing current pulses were injected into Ds during searching (labels as in *B*). The amplitude of the change in membrane potential resulting from current injection is smaller during searching extension cycle onset (left-most arrow) than when Ds is not inhibited (right-most arrow) or when the leg was not moving before or after searching (not shown). For comparison, the right-most arrow points to a membrane potential change that is approximately the same amplitude that resulted from control pulses when the leg was not moving. Middle arrow indicates decrease in potential change that may result from conductance changes associated with action potentials; these type of events were not used in analysis. Scale bar for *B* and *C*: 250 ms, 30 mV.

The T2 leg searching motor pattern can be readily distinguished from walking using extracellular Ds and SETi records and visually observing leg movements making it possible to identify ongoing behaviors in absence of detailed joint kinematics (Fig. 8, *A* and *B*) (Tryba and Ritzmann 2000). The onset of the extension cycle during searching characteristically involves high-frequency SETi activity accompanied by fast extensor tibia (FETi) spikes (Fig. 8*B*) (Tryba and Ritzmann 2000). As with the high-frequency SETi feature at the end of stance phase of walking, during searching this activity begins at a time when there is little or no Ds activity present (Fig. 8*B*) (Tryba and Ritzmann 2000). Accordingly, Ds is inhibited at the onset of the extension cycle during searching when there is high-frequency SETi activity (Fig. 10*A*; $n = 4$ cockroaches, $n = 31$ searching leg movements).

CONDUCTANCE CHANGE ASSOCIATED WITH INHIBITION OF Ds AT SEARCH EXTENSION ONSET. At the onset of each searching extension cycle, Ds is inhibited at the initiation of the high-frequency SETi burst (Fig. 10*B*). This Ds inhibition could result from a decreasing conductance (e.g., to Na^+, or Ca^{2+}) or an increase in conductance (e.g., to K^+ or Cl^-). To test whether Ds inhibition at onset of searching results from a change in conductance, we injected 0.25 nA hyperpolarizing square wave current pulses of brief duration (20 ms) into Ds during searching movements. As a control, we also injected the same amplitude and duration hyperpolarizing current pulses when the glass plate was pitched away from the tethered animal but the animal was not moving its legs. We compared the peak amplitude of the change in membrane potential re-

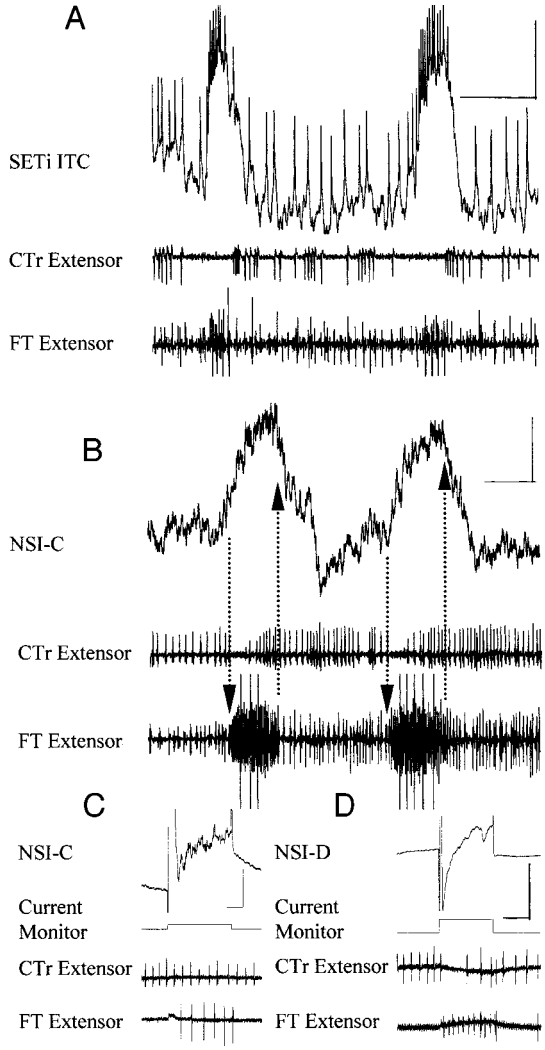

FIG. 11. *A*: SETi intracellular activity and CTr and FT extensor EMGs during tethered semi-intact searching. Note that SETi high-frequency activity during searching is associated with a plateau-like potential, reminiscent of that observed at the end of stance phase of walking (compare with Fig. 9*C*). Scale bar: 200 ms, 10 mV. *B*: activity of nonspiking interneuron-C (NSI-C) and CTr and FT extensor EMGs during tethered searching. Note that NSI-C is rapidly depolarized (downward arrows) at about the same time there is onset of high-frequency SETi activity during searching. NSI-C is rapidly repolarized (upward arrows) when SETi high-frequency activity terminates. Scale bars: 100 ms, 5 mV. *C*: depolarizing current injection (2 nA) into NSI-C when the animal was not moving its legs, resulted in an increase in SETi EMG activity (*bottom*), while Ds activity did not appear to change. Scale bar: 100 ms, 20 mV. *D*: injection of depolarizing current (5 nA) into a nonspiking interneuron (NSI-D) when the animal was not moving its legs resulted in an increase in SETi frequency (FT extensor) and decrease in Ds activity (CTr extensor). Scale bar: 200 ms, 20 mV.

sulting from current injection during searching onset and when the animal was not moving its legs.

During searching, there was a 27.1% decrease in the change in membrane potential that resulted from current injection as compared with control pulses injected either before or after searching ($n = 18$ control pulses, 10 test pulses; Fig. 10*B*). We combined control measurements before and after searching in our analysis to ensure that the perceived increase in conductance was not due to changes in the quality of the recording. We made certain not to include test pulse measurements that occurred during ongoing spiking (Fig. 10*C*). Instead, we measured test pulses at search onset during Ds inhibition (Fig. 10*C*). Similar results were recorded in another animal in which there was a 20.5% smaller change in membrane potential resulting from injected current at the onset of searching than when the animal was not making leg movements. The data suggest that the decrease in Ds activity is the result of direct synaptic activity. They also suggest that the recorded voltage deflections are not the result of electrode movement during ongoing behavior (see also METHODS).

HIGH-FREQUENCY SETi ACTIVITY AT ONSET OF THE EXTENSION PHASE OF SEARCHING. Coupled with Ds inhibition, each extension cycle of searching is also associated with high-frequency SETi activity often accompanied by FETi spikes (Tryba and Ritzmann 2000) (Fig. 11*A*). We recorded intracellularly from SETi while T2 legs engaged in searching. At the beginning of the extension search cycle, SETi is rapidly depolarized above rest and exhibits high-frequency activity (13 search cycles, $n = 2$ animals) (Fig. 11*A*).

We recorded from a nonspiking interneuron (NSI-C) that depolarizes during searching at the time that the SETi high-frequency activity occurs. NSI-C is rapidly depolarized about the same time as SETi high frequency starts (Fig. 11*B*) and begins to repolarize at about the same time SETi high frequency ceases (Fig. 11*B*). Depolarization of NSI-C results in an increase in SETi EMG activity but does not appear to modulate Ds activity (Fig. 11*C*). We also recorded from another NSI, referred to as NSI-D. Depolarizing current injection when the animal was not moving its legs suggested that NSI-D directly or indirectly excited SETi while inhibiting Ds (Fig. 11*D*).

DISCUSSION

The results of this study indicate that the different phase relationships of CTr and FT joints at the onset of extension during searching and at the end of the stance phase of walking result from direct inhibition of the CTr extensor (Ds) and excitation of FT extensor (SETi) motor neurons. Thus these data provide a clear link between intracellular events in the motor neurons and the execution of behaviors. The observed intracellular events can account for the reversal in delay between CTr and FT extension that occurs when the animal switches between walking and searching (Figs. 2*A*, 8, *A* and *B*, and 10*A*). They can also account for the relative timing of the termination of CTr and FT extension at the end of the stance phase of walking (Fig. 2*A*).

The data support the hypothesis that both phasic inhibition and phasic depolarization contribute to extensor motor neuron activity during walking. In contrast, Buschges (1998) suggested that in insects, fictive motor neuron activity is primarily patterned by tonic excitation coupled with phasic inhibition. We will propose possible reasons for this discrepancy. Finally, our data showed that a characteristic feature of Ds activity during the *Blaberus* step cycle, a decline in frequency from peak firing rate near the time of foot set-down, is unlikely to result from sensory feedback due to substrate contact.

Comparison of intact-tethered, semi-intact tethered, and treadmill walking

In the companion paper (Tryba and Ritzmann 2000), we established the behavioral relevance of the intact tethered walking preparation by comparing (CTr and FT) joint kinematics and extensor EMG pattern (Ds and SETi) with those of freely behaving animals. We did not have enough kinematic data collected at the same walking rate from the semi-intact tethered preparation and treadmill preparation to quantitatively compare joint kinematics as was done for T2 tethered versus treadmill data (Tryba and Ritzmann 2000). Nonetheless we briefly tested the behavioral relevance of the semi-intact preparation by examining the occurrence of extensor motor-neuron potentials (Ds and SETi) within a burst and within a (CTr or FT) joint cycle (see Tryba and Ritzmann 2000). The EMG data shown in Fig. 4, *A–C* of Tryba and Ritzmann (2000), were data collected from a semi-intact preparation during an intracellular recording of Ds by methods described in this paper. These data were consistent with similar data sets collected during treadmill (Watson and Ritzmann 1998a) and intact tethered walking (Tryba and Ritzmann 2000), suggesting the semi-intact preparation yields biologically relevant walking data.

The slope of the relationship between mean EMG potentials and joint velocity was higher for semi-intact than for intact tethered data but was lower than for treadmill walking (Tryba and Ritzmann 2000). At least two hypotheses can account for the difference in intact tethered and semi-intact tethered walking data. First, in contrast to intact tethered animals, the semi-intact walking data included some steps where there were fast muscle potentials (Fig. 2*A*), and these may have contributed to a higher joint angular velocity than when only slow motor neurons were active. However, CTr data shown in Fig. 2*B* included only two cycles where Df was active. Even in those cases, it does not appear that there are data points that include a sudden increase in joint velocity at a given EMG frequency (Fig. 2*B*). Therefore it is unlikely that an increase in the slope of the relationship between mean EMG frequency and joint velocity for semi-intact tethered animals can be completely explained by the occurrence of fast motor neuron activity during some of the steps (see also Watson and Ritzmann 1998b).

There is a second possible reason for the difference between intact and semi-intact animals. Tethered walking in both cases may involve an increase in retraction resistance and a reduction in the contribution of whole body inertia to walking (Tryba and Ritzmann 2000). Compared with intact tethered animals, semi-intact tethered animals were more rigidly tethered and had a lower body mass due to evisceration. Both of these factors may reduce loading of the legs and thereby decrease the retraction resistance in the semi-intact versus intact tethered animals. One would then expect the slope of the relationship for mean EMG activity and joint velocity for semi-intact animals to be higher than the intact tethered animals yet lower than what was

observed for treadmill walking, and that is what was found (Fig. 2, *B* and *C*).

Ds and SETi activity during stance phase of walking

During walking, Ds exhibited plateau-like potentials throughout a burst, whereas SETi did so primarily during high-frequency activity at the end of the burst (Figs. 2*A* and 7*A*). We were not able to provide critical evidence that these plateau-like potentials result from active membrane properties rather than summation of depolarizing synaptic input. However, in a reduced preparation, it has been demonstrated that Df can produce plateau potentials triggered as the result of sensory input (Hancox and Pitman 1991, 1993). Therefore there is reason to suspect that the slow motor neuron plateau-like potentials observed during tethered walking are the result of active membrane properties of the motor neuron. If this is the case, then the membrane properties of the extensor motor neurons may in part be responsible for the intraburst frequency characteristics observed during walking, but further study is needed to address this issue.

Evidence from fictive locomotion in stick insects suggests that inhibitory input plays a major role in shaping rhythmic motor activity (Buschges 1998). Our data support the hypothesis that inhibition contributes to termination of motor neuron bursts as was the case for fictive locomotion (Buschges 1998), semi-intact walking (Godden and Graham 1984), and rhythmic leg movements (Pearson and Fourtner 1976). For example, Ds and SETi were depolarized and remained at a depolarized level throughout a burst until the Ds burst and low-frequency SETi activity were terminated at least in part by inhibitory input (Figs. 3*B* and 7*B*). We also recorded from a NSI during walking (NSI-A) whose activity occurred with appropriate timing to periodically inhibit Ds and contribute to burst termination (Fig. 4*C*).

In addition to NSI-A, we recorded from NSI-B, which periodically depolarizes Ds during walking (Fig. 5*B*). These data suggest at least two alternative hypotheses for excitation of Ds activity during walking. First, NSI-B is tonically depolarized and its depolarization is periodically interrupted by inhibition. In that case, one might suspect that inhibition is centrally generated (Buschges 1998) via the flexor burst generator (Pearson 1976; Pearson and Fourtner 1975). Second, there may be an interneuron or interneurons that generate(s) rhythmic excitation of Ds. Our data do not allow us to distinguish between these two alternatives. For example, we were not able to determine whether current injection into NSI-B can reset the phase of extensor motor neuron bursts. However, the data do suggest that extensor motor-neuron bursts do not simply result from direct tonic excitation of the motor neuron, that is, periodically terminated by rhythmic inhibition (see Buschges 1998; Pearson 1976; Pearson and Fourtner 1975). Further, the finding that NSI-B begins to hyperpolarize prior to the end of Ds activity during each step also suggests that a reduction in Ds excitation may contribute to burst termination (Fig. 5*B*).

It is possible that NSI-B activity is the result of sensory feedback. That is, during walking, feedback from sensory cues might depolarize NSI-B, and in turn NSI-B could then depolarize Ds. This is an important issue as current injection into NSI-B had remarkable (direct or indirect) effects on extensor burst duration during walking, and at least one candidate source of sensory information has been shown to modulate stance duration. In particular, activation of load receptors in cockroach legs (campaniform sensilla) and muscle force receptors in vertebrate muscle (Golgi tendon organs) results in excitation of extensor motor neurons and prolongation of stance phase (Cruse 1976; Cruse and Saxler 1980; Duysens and Pearson 1980; Pearson 1976; Whelan et al. 1995). We cannot resolve this issue without considerably more circuitry analysis than we currently have. However, it is worth noting that SETi burst duration appeared to also change when NSI-B was depolarized and hyperpolarized, resulting in prolonged or shortened Ds activity (respectively, Fig. 5, *C* and *D*). Presumably, the effect of shortening or lengthening the burst of the principal leg depressor motor neuron would be to prematurely unload or prolong leg loading during stance. If that is the case, the data indirectly support the hypothesis that afferents signaling leg loading can in part determine extensor burst duration (Whelan et al. 1995). SETi activity may also be influenced by NSI-B activity. Although this effect was not observed during current injection into NSI-B when the animal was not moving its legs (Fig. 5*A*), it might be uncovered during walking (see also Kitmann et al. 1995).

Coordinating the phase relationship of Ds and SETi at the end of stance and during searching

As was the case in this study, Krauthamer and Fourtner (1978) noted that SETi activity is maximally excited at the end of stance phase at the same time that Ds activity declines. We can only speculate that the function of this high-frequency SETi activity is to maintain stance phase support at a time when CTr extensor force would be expected to decline (Fig. 2*A*) (see also Krauthamer and Fourtner 1978). Our data predict that coordination of Ds and SETi at the end of stance phase involves recruitment of interneuron(s) that provide inhibitory drive to Ds and also depolarize SETi at the end of stance (Figs. 3, *B* and *C*, and 9, *C* and *D*). Although not recorded during searching or walking, we found one nonspiking interneuron (NSI-D) that depolarizes SETi and inhibits Ds and could serve this function (Fig. 11*D*). If this hypothesis is correct, one would expect to observe high-frequency SETi activity at the end of stance resulting from phasic depolarization that appears to be independent of that generating the SETi burst concurrent with Ds excitation throughout much of stance, and that is what we found (Figs. 9*D*). The fact that there is continuation of low-frequency Ds activity following interruption of the Ds burst at the same time that high-frequency SETi activity occurs also supports this hypothesis (Fig. 9*D*). Along these lines, inhibitory input leading to burst termination appears to be independent of Ds inhibition that is concurrent with high-frequency SETi activity and termination of SETi high-frequency activity (Figs. 9*D* and both 9*C* and 7*B*).

We found that there are components of extensor motor neuron coordination that appear to occur during both walking and searching. The data are consistent with a modular organization of multi-joint control whereby individual interneurons(s) may coordinate extensor motor neurons during searching and walking. The recruitment of modules to coordinate multiple joints during an ongoing rhythmic behavior has also been proposed to occur during rostral scratch in the turtle and

is evident during a variant of rostral scratch termed "extensor deletion" (Robertson and Stein 1988). Thus use of a modular neural architecture may represent a general way of coordinating movements at multiple joints.

In stick insects, a population of interneurons coordinates the activity of motor neurons acting at several joints (Kitmann et al. 1995). The activity of each interneuron either opposes or supports an ongoing behavior. While the neural architecture underlying many behaviors is distributed there is evidence that in stick insects, "constant functional elements" or "modules" of the distributed network are recruited to coordinate multiple joints during both rhythmic and nonrhythmic behaviors (i.e., searching, walking, rocking and postural reflexes) (Kitmann et al. 1995). Further, NSIs that are homologous to those identified in stick insects exist among other insects (Wolf and Buschges 1995), so it is likely that similar interneurons are represented and serve to coordinate motor activity at multiple joints in cockroaches. In fact, we recorded from some interneurons that may function to coordinate extensor motor activity at the CTr and FT joints (Figs. 4, 5, and 11, *B–D*). Although there may be exceptions, in stick insects, current injection into all of the studied interneurons had similar effects on motor activity when injected prior to leg movements as it did when the animal engaged in a variety of behaviors (Kitmann et al. 1995). Therefore although we did not record from NSI-D during walking and searching, it is reasonable to suspect that it functions to inhibit Ds and excite SETi during those behaviors as it did when the animal was not moving its legs (Fig. 11*D*).

Our data suggest that interneuron(s) contributing to simultaneous SETi depolarization and Ds inhibition may coordinate the activity of these motor neurons at the end of stance and the onset of the searching extension phase. During walking, "recruitment" of such interneurons may in fact result from additional activation of a subpopulation of nonspiking interneurons whose ongoing activity is modulated by central pattern generators (see also Kittmann et al. 1995). Along these lines, we found there was a rapid increase in depolarization of NSI-A at the termination of Ds activity that appeared to occur in addition to ongoing rhythmic oscillation of its membrane potential during walking (Fig. 4*C*) (see also Kitmann et al. 1995).

As is the case for stick insects (Kittmann et al. 1995), a distributed population of interneurons is likely to coordinate multiple joints during walking and searching in cockroaches. We recorded from one NSI that contributed to depolarization of SETi during searching without influencing Ds activity (NSI-C; Fig. 11, *B* and *C*). These data suggest that there is a population of cells that are recruited to coordinate Ds and SETi activity during the extension phase of searching. This population may be recruited in parallel with interneurons involved in multi-joint coordination, or they may represent an overlapping group of cells that are recruited by interneurons involved in simultaneously coordinating motor neurons acting at multiple joints (see also Kittmann et al. 1995).

Relationship of motor neuron activity to joint kinematics and foot contact

We tested several hypotheses regarding the induction of Ds high-frequency activity before foot set-down and its decline during stance phase of walking. Afferent input from tarsal contact does not appear to be responsible for the characteristic decline in Ds activity that occurs near foot set-down during walking (Fig. 6). Similar conclusions came from experiments on cats in which a decline in ankle extensor EMG activity still occurred in absence of substrate contact during walking (Gorassini et al. 1994). Therefore either different afferent pathways such as joint movement and position information may play a role or this EMG component is centrally generated as has been suggested for cats (Hiebert et al. 1994). Our data suggest that it is possible that sensory cues from joint angle receptors initiate the decline in Ds high-frequency activity, although this hypothesis needs to be tested further (see also Watson and Ritzmann 1998a). We also examined whether particular CTr and FT joint angles are correlated with the onset of high-frequency SETi activity. Our data suggested that the onset of high-frequency SETi activity is not initiated when the CTr and FT joints extended to a particular joint angle. These data further suggest that central influences and/or other sensory cues may initiate Ds inhibition associated with high-frequency SETi activity.

Conclusion

This study was initiated by observing distinct behavioral changes in leg movements when a cockroach switches from walking to searching (Tryba and Ritzmann 2000). At the level of motor neurons, we can now account for the principal mechanisms (Ds inhibition concurrent with SETi excitation) that are responsible for the phase relationship of the CTr and FT joints during the extension phase searching. Similar mechanisms were found to coordinate these motor neurons during the end of stance during walking. In both cases, our data indirectly support the modular concept of multi-joint coordination. We additionally found evidence that searching and walking extensor motor neuron activity results from the combined input of a population of interneurons.

The authors thank Drs. Sasha N. Zill and Joanne Westin for very helpful comments on the manuscript and Dr. James T. Watson for use of his T2 leg treadmill walking data for comparison and helpful comments. Thanks to A. Pollack for technical support.

This work was supported by Office of Naval Research Grant N0014-99-1-0378 to R. E. Ritzmann.

Present address and address for reprint requests: A. K. Tryba, Dept. of Organismal Biology and Anatomy, The University of Chicago, Anatomy Bldg., 1027 E. 57th St., Chicago, IL 60637.

E-mail: Tech10S@techsan.org

Received 29 November 1999; accepted in final form 13 March 2000.

REFERENCES

ANGEL MJ, GUERTIN P, JIMENEZ I, AND MCCREA DA. Group I extensor afferents evoke disynaptic EPSPs in cat hindlimb extensor motorneurons during fictive locomotion. *J Physiol (Lond)* 494: 851–861, 1996.

BASSLER U. The walking- (and searching) pattern generator of stick insects, a modular system composed of reflex chains and endogenous oscillators. *Biol Cybern* 69: 305–317, 1993.

BRUNN DE. Cooperative mechanisms between leg joints of *Carausius morosus*. I. Nonspiking interneurons that contribute to interjoint coordination. *J Neurophysiol* 79: 2964–2976, 1998.

BURROWS M. The control of sets of motorneurons by local interneurons in the locust. *J Physiol (Lond)* 298: 213–233, 1980.

BURROWS M. Local interneurons in insects. In: *Neurones Without Impulses*, edited by Roberts A and Bush BMH. Cambridge UK: Cambridge Univ. Press, 1981, p. 199–221.

BURROWS M AND MATHESON T. A presynaptic gain control mechanism among sensory neurons of a locust leg proprioceptor. *J Neurosci* 14: 272–282, 1994.

BUSCHGES A. Inhibitory synaptic drive patterns motorneuronal activity in rhythmic preparations of isolated thoracic ganglia in the stick insect. *Brain Res* 783: 262–271, 1998.

BUSCHGES A, KITMANN R, AND SCHMITZ J. Identified nonspiking interneurons in leg reflexes and during walking in the stick insect. *J Comp Physiol [A]* 174: 685–700, 1994.

BUSCHGES A, SCHMITZ J, AND BASSLER U. Rhythmic patterns in the thoracic nerve cord of the stick insect induced by pilocarpine. *J Exp Biol* 198: 435–456, 1995.

CATTAERT D, EL MANIRA A, AND CLARAC F. Direct evidence for presynaptic inhibitory mechanisms in crayfish sensory afferents. *J Neurophysiol* 67: 610–624, 1992.

CATTAERT D, EL MANIRA A, MARCHAND A, AND CLARAC F. Central control of the sensory afferent terminals from a leg chordotonal organ in crayfish in vitro preparation. *Neurosci Lett* 108: 81–87, 1990.

CRUSE H. The function of the legs in the free walking insect, *Carausis morosus*. *J Comp Physiol* 112: 235–262, 1976.

CRUSE H AND SAXLER G. Oscillations in force in the standing legs of walking insect (*Carausius morosus*). *Biol Cybern* 36: 159–163, 1980.

DUYSENS J AND PEARSON KG. Inhibition of flexor burst generation by loading ankle extensor muscles in walking cats. *Brain Res* 187: 321–332, 1980.

EL MANIRA A, CATTAERT D, AND CLARAC F. Monosynaptic connections mediate resistance reflex in crayfish (*Procambarus clarkii*) walking legs. *J Comp Physiol [A]* 168: 337–349, 1991.

ENGBERG I AND LUNDBERG A. An electromyographic analysis of muscular activity in the hindlimb of the cat during unrestrained locomotion. *Acta Physiol Scand* 75: 614–630, 1969.

GODDEN DH AND GRAHAM D. A preparation of the stick insect *Carausius morosus* for recording intracellularly from identified neurones during walking. *Physiol Entomol* 9: 275–286, 1984.

GORASSINI MA, PROCHAZKA A, HIEBERT GW, AND GAUTHIER MJA. Corrective responses to loss of ground support during walking. I. Intact cats. *J Neurophysiol* 71: 603–610, 1994.

GRAHAM D AND BASSLER U. Effects of afference sign reversal on motor activity in walking stick insect (*Carausius morosus*). *J Exp Biol* 91: 179–193, 1981.

GRILLNER S AND ZANGGER P. On the central generation of locomotion in the low spinal cat. *Exp Brain Res* 43: 241–261, 1979.

HANCOX JC AND PITMAN RM. Plateau potentials drive axonal impulse burst in insect motorneurons. *Proc R Soc (Lond) B Biol Sci* 244: 33–38, 1991.

HANCOX JC AND PITMAN RM. Plateau potentials in an insect motorneurone can be driven by synaptic stimulation. *J Exp Biol* 176: 307–310, 1993.

HESS D AND BUSCHGES A. Sensory pathways involved in interjoint reflex action of an insect leg. *J Neurobiol* 33: 891–913, 1997.

HESS D AND BUSCHGES A. Role of proprioceptive signals from an insect femur-tibia joint in patterning motorneuronal activity of an adjacent joint. *J Neurophysiol* 81: 1856–1865, 1999.

HIEBERT G, GORASSINI MJW, PROCHAZKA A, AND PEARSON KG. Corrective responses to loss of ground support during walking. II. Comparison of intact and chronic spinal cats. *J Neurophysiol* 71: 611–622, 1994.

HISADA M, TAKAHATA M, AND NAGAYAMA T. Local non-spiking interneurons in the arthropod motor control systems: characterization and their functional significance. *Zool Sci* 1: 681–700, 1984.

HOYLE G AND BURROWS M. Neural mechanisms underlying behavior in the locust *Schistocera gregaria*. I. Physiology of identified motorneurons in the metathoracic ganglion. *J Neurobiol* 4: 3–41, 1973.

KITMANN R, SCHMITZ J, AND BUSCHGES A. Premotor interneurons in generation of adaptive leg reflexes and voluntary movements in stick insects. *J Neurobiol* 31: 512–531, 1995.

KRAUTHAMER V AND FOURTNER CR. Locomotory activity in the extensor and flexor tibiae of the cockroach, *Periplaneta americana*. *J Insect Physiol* 24: 813–824, 1978.

PEARSON K. The control of walking. *Sci. Am.* 235: 72–74, 79–82, 83–86, 1976.

PEARSON KG AND FOURTNER CR. Nonspiking interneurons in walking system of the cockroach. *J Neurophysiol* 38: 33–51, 1975.

PEARSON KG AND ILES JF. Innervation of coxal depressor muscle in the cockroach, *Periplaneta americana*. *J Exp Biol* 54: 215–232, 1971.

RAMERIZ JM AND PEARSON KG. Octopamine modulation of interneurons in the flight system of the locust. *J Neurophysiol* 66: 1522–1537, 1991.

ROBERTSON GA, MORTIN LI, KIEFER J, AND STEIN PSG. Three forms of the scratch reflex in the spinal turtle: central generation of motor pattern. *J Neurophysiol* 53: 1517–1534, 1985.

ROBERTSON GA AND STEIN PSG. Synaptic control of hindlimb motoneurones during three forms of the fictive scratch reflex in the turtle. *J Physiol (Lond)* 404: 101–128, 1988.

RYCKEBUSCH S AND LAURENT G. Rhythmic patterns evoked in locust leg motor neurons by the muscarinic agonist pilocarpine. *J Neurophysiol* 69: 1583–1595, 1993.

SAUER AE AND BUSCHGES A. Presynaptic inhibition of afferents—a mechanism influencing gain in proprioceptive feedback systems. In: *Gottingen Neurobiology Report*, edited by Elsner N and Breer H. Stuttgart: Verlag, 1994, p. 283.

SCHMITZ J, BUSCHGES A, AND KITTMANN R. Intracellular recordings from nonspiking interneurons in a semiintact, tethered walking insect. *J Neurobiol* 22: 907–992, 1991.

SIEGLER MVS. Nonspiking interneurons and motor control in insects. *Adv Insect Physiol* 18: 249–304, 1985.

SILLAR KT, AND SKORUPSKI P. Central input to primary afferent neurones in crayfish. *Pacifastus leniusculus* is correlated with rhythmic output of thoracic ganglia. *J Neurophysiol* 55: 678–688, 1986.

TRYBA AK AND RITZMANN RE. Multi-joint coordination during walking and foothold searching in the *Blaberus* cockroach. I. Kinematics and electromyograms. *J Neurophysiol* 83: 3323–3336, 2000.

WALLEN P. Phasic control of vertebrate motoneurons during rhythmic motor acts with special reference to fictive locomotion in the lamprey. In: *Neurobiology of Vertebrate Locomotion*, edited by Grillner S, Stein PSG, Stuart DG, Forssberg H, and Hermann RM. Basingstoke: Macmillan, 1986, p. 307–319.

WATSON JT AND RITZMANN RE. Leg kinematics and muscle activity during treadmill running in the cockroach, *Blaberus discoidalis*. I. Slow running. *J Comp Physiol [A]* 182: 11–22, 1998a.

WATSON JT AND RITZMANN RE. Leg kinematics and muscle activity during treadmill running in the cockroach, *Blaberus discoidalis*. II. Fast running. *J Comp Physiol [A]* 182: 22–33, 1998b.

WHELAN PJ, HIEBERT GW, AND PEARSON KG. Stimulation of group I extensor afferents prolongs the stance phase in walking cats. *Exp Brain Res* 103: 20–30, 1995.

WILSON JA AND PHILLIPS CE. Pre-motor non-spiking interneurons. *Prog Neurobiol* 20: 98–107, 1983.

WOLF H. Activity patterns of inhibitory motoneurones and their impact on leg movement in tethered walking locusts. *J Exp Biol* 152: 281–304, 1990.

WOLF H AND BUSCHGES A. Nonspiking local interneurons in insect leg motor control. II. Role of nonspiking local interneurons in the control of leg swing during walking. *J Neurophysiol* 73: 1861–1875, 1995.

WOLF H AND BURROWS M. Proprioceptive sensory neurons of a locust receive rhythmic presynaptic inhibition during walking. *J Neurosci* 15: 5623–5636, 1995.

WOLF H AND PEARSON KG. Intracellular recordings from interneurons and motoneurons in intact flying locusts. *J Neurosci Methods* 21: 345–354, 1987.

ZERNICKE RF AND SMITH JL. Biomechanical insights into neural control of movement. In: *Handbook of Physiology*. New York: Oxford University, 1996, sect. 12, p. 293–330.